Sub Topic: Fire

13th U.S. National Combustion Meeting
Organized by the Central States Section of the Combustion Institute
March 19-22, 2023
College Station, Texas

Examining the effectiveness of water suppression for mitigating backdrafts

Ryan Falkenstein-Smith[1,*] *and Thomas Cleary*[1]

[1]*National Institute of Standards and Technology, Gaithersburg, MD, USA*
[*]*Corresponding author:* ryan.falkenstein-smith@nist.gov

Abstract: An analysis of the backdraft phenomenon's mitigation due to water suppression is conducted in a 2/5th scale compartment. Different volumes of water were introduced via a ceiling-mounted misting nozzle into the compartment, which hosted conditions conducive to backdraft (i.e., a fuel-rich, oxygen-depleted, and high-temperature environment). The effect of water suppression was examined using two metrics indicative of backdraft: 1) the flow of the gravity current mixing into the compartment and 2) the total heat release of the resulting fireball. The gravity current was analyzed using density estimations obtained from phi meter measurements at six positions within the compartment. The total heat release of each observed backdraft was estimated from carbon dioxide and carbon monoxide concentrations in the exhaust duct residing over the compartment. Backdrafts were still observed in instances where water suppression was implemented. In some cases, water suppression increased fuel concentration around designated ignition sources. Upon entering the compartment, the gravity current's velocity declined as more water was introduced, allowing more fuel to escape and less to be combusted in the ensuing fireball. Measurements were validated through comparisons to established empirical formulas and orthogonal measurements.
Keywords: Backdraft, Water Suppression, Gravity Current, Total Heat Release

1. Introduction

A backdraft is a deflagration resulting from the rapid introduction of air driven via a gravity current to an oxygen-depleted, fuel-rich, and heated compartment, which then combusts [1]. When suspecting a backdraft at a fire scene, a firefighter may implement risk mitigation techniques such as venting the roof or penciling at the ceiling with a straight water stream [2, 3]. These methods aim to evacuate the heat and unburned fuel within the enclosure, creating safer and cooler conditions and eliminating the potential of backdraft.

Many researchers have examined the physical mechanisms conducive to backdraft phenomenon [3–9]. Fleishmann demonstrated the significance of the gravity current and how mixing within an enclosure creates favorable conditions for backdraft [10–12]. Gottuk highlighted the impact of water suppression by investigating how diluting an enclosure with significant volumes of water offsets the likelihood of backdraft [13, 14]. Other works have established critical factors that impact the risk of backdrafts, such as fuel type, compartment size, and ventilation [15–18].

Many of these studies have been informative in developing mitigation tactics to prevent backdrafts when suspected. In this work, an enhanced phi meter is implemented to investigate the effects of water suppression in an enclosure on the physical mechanisms conducive to the backdraft phenomenon. A series of experiments involving gas mixture composition measurements

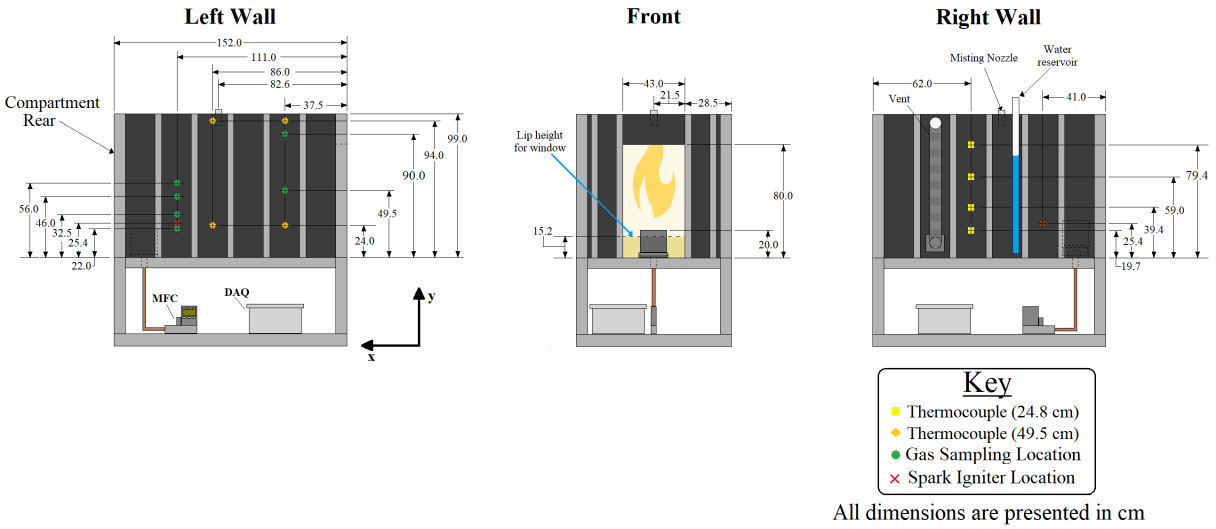

Figure 1: Schematic of the $2/5^{\text{th}}$ scale compartment utilized for backdraft experiments. The relative uncertainty of the presented dimensions was estimated to be less than 1%.

collected at various positions within a $2/5^{\text{th}}$ scale compartment is examined. The measurements obtained using different amounts of water introduced into the compartment demonstrate the impact of the suppression technique on the mixing of the gravity current within the compartment and the resulting intensity of the backdraft when observed.

2. Methods/Experimental

2.1 Compartment design and measurements

Experiments were conducted in an enclosure, $2/5^{\text{th}}$ the dimensions of an ASTM test room. A schematic of the compartment and various measurement locations is provided in Fig. 1. In some experiments, the compartment opening was modified using a steel plate, providing a "window" opening configuration and reducing the opening size by approximately 20.0 %. A description of the compartment design is detailed in Ref. [19].

Experiments were initiated when the nominally square sand burner, with a characteristic length of 17.8 cm, was ignited at the back of the compartment. This campaign implemented two subsets of experiments utilizing a 37.5 kW $\pm$ 1.0 kW methane fire or a 25.0 kW $\pm$ 1.0 kW propane fire. After igniting, the flame was allowed to burn for 60.0 s with the compartment door opened, and afterward, the door was shut. While isolated, fuel continued to be fed into the sand burner for 300 s after the ignition. The doorway was opened 330 s after burner ignition. When the door opened, a spark ignitor, located 25.4 cm from the compartment floor, was charged, potentially resulting in a backdraft. The timing of the events in the experimental procedure was based on conditions known from Ref. [20] to generate backdrafts robustly.

Water suppression was implemented via a misting nozzle on the compartment's ceiling, approximately 82.6 cm from the door and 50.0 cm from either side wall. The misting nozzle used in this work was a brass full cone nozzle with a spray angle of 90° and a nominally 1.0 mm orifice diam-

eter. The compartment's exterior right wall housed a water reservoir maintained at approximately 103421 Pa which could produce a steady stream for 45.0 s for a total volume of approximately 400 ml $\pm$ 20 ml of water. The spray time was varied between 0 s to 44.0 s in increments of 11.0 s and was implemented such that spray time concluded at 300 s from burner ignition.

Temperature measurements were obtained from an array using 49.5 cm long Type K thermocouples configured in a line on a wall adjacent to the compartment opening. The thermocouples were spaced approximately 19.9 cm apart. A pressure tap was positioned in the center of the opposing wall of the thermocouple array. All pressure and temperature measurements were sampled at 1.0 Hz using a data acquisition system (DAQ) during each experiment, except for 20.0 s prior and 40.0 s after an anticipated backdraft when the sampling rate increased to 25.0 Hz. The sampling rate was increased from a 1.0 min period to resolve the rapid dynamics during a backdraft.

2.2 Gas mixture composition measurements

Gas mixture measurements were examined at two locations within the compartment for each experiment. Three sets of different locations were selected as positions of interest.

1. In the upper (y = 94.0 cm) and middle (y = 49.5 cm) layer of the compartment 37.5 cm from the compartment opening and approximately 50.0 cm $\pm$ 2.0 cm from the sidewall of the compartment

2. Approximately 5.0 cm above (y = 56.0 cm) and below (y = 46.0 cm) the middle spark ignitor (y = 50.7 cm) 111.0 cm away from the compartment opening and approximately 50.0 cm $\pm$ 2.0 cm from the sidewall of the compartment

3. Approximately 7.0 cm above (y = 32.5 cm) and 3.0 cm below (y = 22.0 cm) the low spark ignitor (y = 25.4 cm) 111.0 cm away from the compartment opening and approximately 50.0 cm $\pm$ 2.0 cm from the sidewall of the compartment

Extracted gas samples were portioned into a gas analyzer, a phi meter, and a 300.0 ml stainless steel reservoir fitted with baffles and a vacuum pump. The gas analyzer was equipped with paramagnetic and two nondispersive infrared sensors to measure the extracted gas' oxygen, carbon dioxide, and carbon monoxide concentrations. A chiller was placed upstream of the gas analyzer to preserve its integrity, signifying that all of its measurements were conducted on a dry basis.

The phi meter [21, 22] was implemented to evaluate the equivalence ratio of the extracted gas sample. The phi meter design provides real-time equivalence ratio measurements without knowledge of fuel composition. Additional details regarding the phi meter design and application are described in Ref. [22].

The stainless-steel reservoir was used to collect well-mixed gas samples that were analyzed using an Agilent 5977E Series Gas Chromatograph[1] with thermal conductivity and mass selectivity detectors (GC/MSD) to estimate time-averaged gas species concentrations [23–26]. Gas samples were extracted through a sampling line via a vacuum pump for 1.0 min, initiated 70.0 s before the door opened. Time-averaged species concentration measurements were estimated to represent an extracted gas mixture obtained 20.0 s before the door opened.

[1]Certain commercial products are identified in this work to specify adequately the equipment used. Such identification does not imply a recommendation by the authors, nor does it imply that this equipment is the best available for the purpose.

Sample lines feeding into the phi meter and stainless-steel reservoir were heated (approx. 90.0 °C ± 5.0 °C) using heating tape. Heating the sampling line was essential to account for water vapor in the extracted gas sample. Oxygen concentrations in the paramagnetic sensor and phi meter data were recorded at 1.0 Hz throughout the experiment using a DAQ.

2.3 Heat release measurements

For each experiment, the compartment was positioned under a 3.0 MW calorimeter (6.0 m canopy hood) [27]. In instances where a backdraft event was observed, the total heat release was calculated using Eq. 1, which utilizes carbon dioxide generation calorimetry with a correction for carbon monoxide generation. Typically, total heat release calculations are obtained via oxygen consumption calorimetry. In this series of experiments, however, large amounts of unburned hydrocarbon fuels in the exhaust presented an error for oxygen consumption calorimetry since it is unaccounted for in the sampling train.

$$THR = \sum_{t=0}^{\infty} \left[\dot{m}_{CO_2}(t) \left(\frac{\mathrm{LHV_F\ MW_F}}{\mathrm{x\ MW_{CO_2}}} \right) + \dot{m}_{CO}(t) \left(\frac{\mathrm{LHV_F\ MW_F}}{\mathrm{x\ MW_{CO}}} - \Delta \mathrm{H^o_{C,CO}} \right) \right] \Delta\, t \qquad (1)$$

Here, $\dot{m}_{CO_2}(t)$ and $\dot{m}_{CO}(t)$ represent the mass flow rate of CO_2 and CO measured in the duct, respectively. The number of carbon atoms and lower heating value of the parent fuel are represented by x and $\mathrm{LHV_F}$, respectively. The molecular weight of the parent fuel, carbon dioxide, and carbon monoxide is denoted as $\mathrm{MW_F}$, $\mathrm{MW_{CO_2}}$, and $\mathrm{MW_{CO}}$, respectively. The heat of combustion for carbon monoxide, $\Delta \mathrm{H^o_{C,CO}}$ used in Eq. 1 is 10.10 kJ/g as reported by Ref. [28]. Data was collected at 1.0 Hz resulting in a time-step, $\Delta\, t$, of 1. The heat released from the combustion gases trapped in the compartment before opening the door is subtracted from the measured total heat released for a backdraft.

2.4 Uncertainty Analysis

The uncertainty analysis of the gas species measurements obtained via phi meter, gas analyzer, and GC/MS are reported in Refs. [20, 22, 23, 29]. The uncertainty of the total heat release measurement is discussed in Ref. [27]. The uncertainty of time-averaged measurements were estimated from a combination of the Type A and B evaluation of uncertainty. The Type A evaluation of uncertainty was estimated from the variance of the averaged measurements. The Type B evaluation of uncertainty was determined from the reported instrumentation error. The uncertainty of calculated parameters was calculated from the law of propagation of uncertainty. The variance between the averaged measurements was determined to be the dominant contributor to the estimated uncertainty. All uncertainties expressed in this work are defined as combined uncertainties with a coverage factor of 2, representing a 95% confidence level.

3. Results and Discussion

3.1 Gravity current

The phi meter's equivalence ratio, combined with the gas analyzer measurements, was used to estimate the gas mixture density within the compartment before the door opened. The unburned fuel

concentration was calculated from the product of the equivalence ratio and oxygen concentration measurements over the stoichiometric coefficient of the parent fuel. The water concentration was estimated from the ratio between the carbon dioxide and carbon monoxide concentration measurements and the carbon-to-hydrogen ratio of the parent fuel. The remaining gas composition was assumed to be inert.

The molecular weight of the gas mixture was calculated from the estimated gas concentrations in two different zones of the compartment. The zones were partitioned at the mid-plane of the compartment, 40.0 cm from the compartment floor. The dividing plane height was estimated from gas concentration measurements observed to be reasonably homogeneous. An average gas concentration was determined from a combination of gas measurements in each zone.

The total zone amount of substances were estimated using the temperature and pressure measurements made throughout the compartment. Temperature measurements were averaged within each zone to obtain an approximate temperature, while the same pressure reading was for both zones. The total zone mass was then determined from the product of the molecular weight and the total amount of substances in their respective zones. The compartment density was calculated from the sum of masses in each zone over the total volume.

The comparison between the water spray time and the estimated density of the gas mixture is shown in Fig. 2. In either case, where methane or propane is used, the estimated internal density determined from gas mixture composition measurements at different locations agrees in the measured and expected cases. The consensus between the estimated and expected density indicates the method used to estimate gas concentrations and zones was appropriate. Figure 2 also shows the decreasing discrepancy between the internal density and the ambient density of the gravity current.

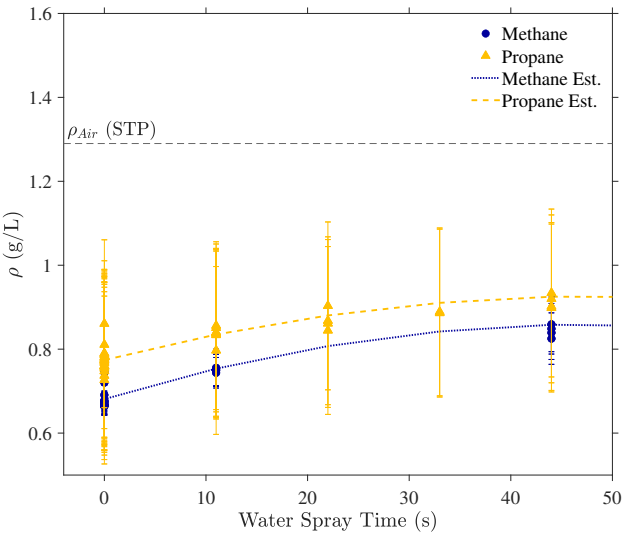

Figure 2: The calculated internal density of the compartment before door opened as a function of water spray time. The uncertainty of the density was estimated from a combination of the Type A and B evaluation of uncertainty.

The relationship between the normalized positive density difference and the observed gravity current velocity is presented in Fig. 3. The dotted line represents the calculated gravity current velocity, $u_{\text{calc.}}$, which was estimated using the relationship between the inertial and gravitational

forces (i.e., Froude number, Fr).

$$Fr = \frac{u_{\text{obsv.}}}{\sqrt{g\ h\ \beta}} \tag{2}$$

As documented in other works [10, 30], the Froude number is determined from the observed velocity of the gravity current, $u_{\text{obsv.}}$ and the product of the gravitational constant, g (9.81 m/s^2), the height of compartment, h (1.0 m), and β, the normalized positive density difference between density within the compartment before the door opened, ρ, and the density of the ambient fluid within the gravity current, ρ_o. In this work, the observed gravity current velocity was estimated from the distance between the compartment opening and the spark ignitor (1.1 m) over the duration from when the compartment door opens to ignition. The time from when the door opens to ignition was determined from video recordings of the compartment opening for experiments where a backdraft occurred.

$$u_{\text{calc.}} \approx \frac{1}{5}\sqrt{g\ h\ \beta} \quad ; \quad \beta = \frac{\rho_o - \rho}{\rho} \tag{3}$$

The average Froude number was approximately 0.2 $\pm$ 0.05, which differs from other values [10, 30] due to the geometry of the opening. The average Froude number was calculated from a combined dataset that included the "door" and "window" configuration data. The different configuration datasets were combined after no statistical significance was determined in a binomial analysis of variance.

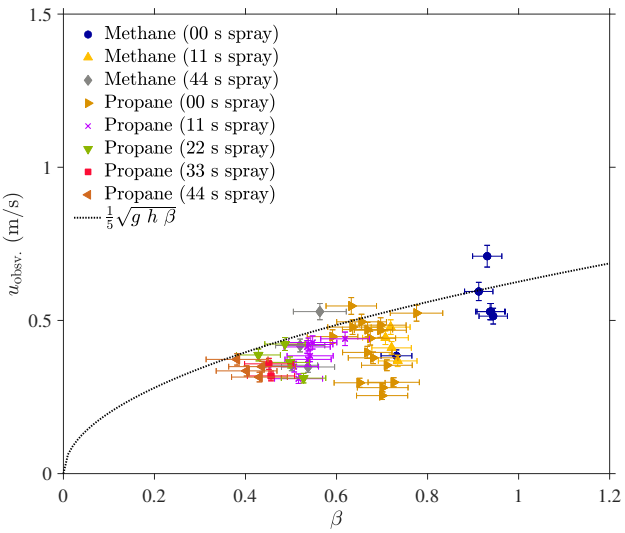

Figure 3: The observed gravity current velocity as a function of the normalized positive density difference. The uncertainty of $u_{\text{obsv.}}$ was estimated from the Type B evaluation of uncertainty. The uncertainty of β was estimated from the law of propagation of uncertainty.

The relationship between the normalized positive density difference and observed gravity current velocity follows the Eq. 3, shown as a dotted line. The agreement between the experimental and calculated velocity suggests that the calculated Froude number is reasonable. The discrepancy between specific experiments may be an erroneous result of the single-view observation used to determine the ignition time.

3.2 Ignition

Backdrafts were observed in most experiments despite applying water suppression. From the extracted gas samples collected around the spark ignitor and analyzed from the GC/MS, the gas mixtures were observed to be flammable or nearly flammable after water suppression was implemented. Figure 4 shows the extracted gas mixture composition presented on a flammability diagram, where CO_2 and H_2O are included within the inert portion. Other fuels detected in the extracted gas sample such as carbon monoxide, ethane, ethylene, acetylene, and propylene were measured in trace amounts and added to the fuel concentration presented here. In experiments with a 44.0 s spray time, the fuel concentration surrounding the spark ignitor increased when using methane or remained relatively constant when using propane. In all experiments, the fuel concentration is high enough such that the path to pure air passes through the flammability region, suggesting that as the gravity current enters the compartment, a combustible mixture is present around the spark ignitor, causing ignition.

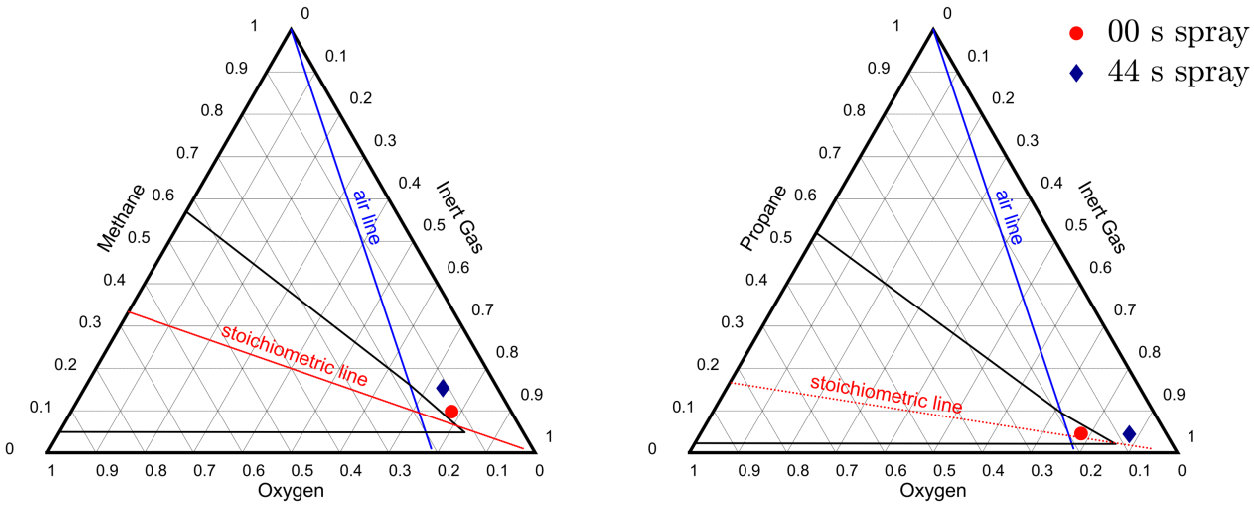

Figure 4: Flammability diagram of gas mixtures surrounding the spark ignitor extracted 10.0 s before the door opened. The 0.0 s and 44.0 s spray times are shown for experiments involving a 37.5 kW methane fire (left) and 25.0 kW propane fire (right) with a fuel flow time of 300 s.

3.3 Backdraft intensity

Water suppression techniques were observed to affect the intensity of the backdraft phenomenon, specifically the total heat release of the exiting flame. The total heat release of observed backdrafts is plotted as a function of the calculated gravity current velocity in Fig. 5. The calculated gravity current velocity is determined from Eq. 3 using the estimated normalized positive density difference. In cases where no water suppression is implemented, the total heat release is shown to approach a critical velocity. The maximum density difference between the fuel and ambient air restricts the total heat release. For the velocity to be close to 1 m/s, the density of the internal gas mixture would have to be half of the air. The total heat release decreases as more water is added to the compartment.

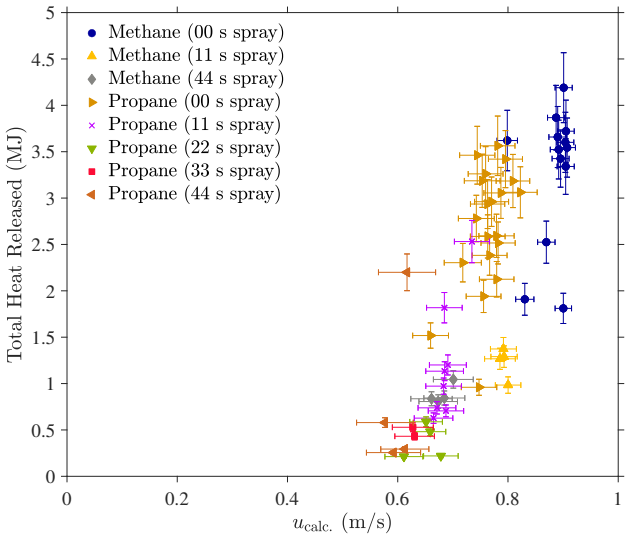

Figure 5: Total heat release of backdrafts plotted as a function of the calculated velocity current. The uncertainty of each measurement was estimated from the law of propagation of uncertainty.

The decline of the total heat release corresponding to the gravity current velocity is attributed to the loss of fuel within the compartment as more air flows into the compartment. Figure 6 presents the estimated fuel mass loss as a function of the gravity current. The fuel loss was calculated from the difference between the total energy content residing within the compartment before the door opened and the measured heat release. The total energy content residing within the compartment before an anticipated backdraft was calculated from the product of the total fuel mass and the heat of combustion of the respective fuel. The uncombusted fuel mass indirectly increases with the calculated gravity current velocity, indicating that as air flows more slowly into the compartment, more fuel is allowed to escape before ignition, resulting in a smaller backdraft.

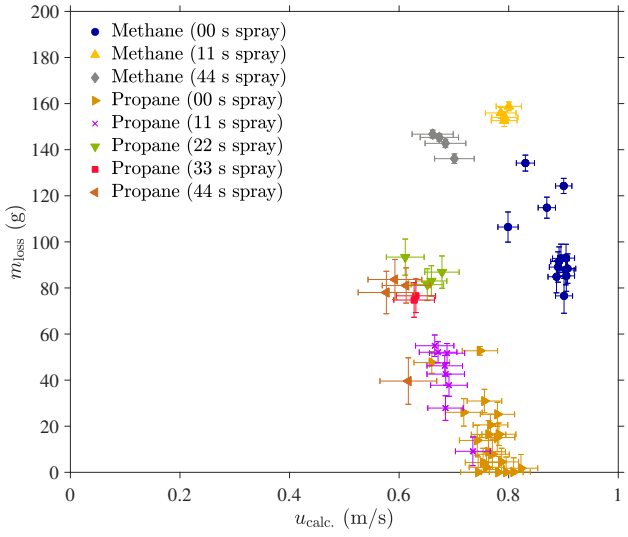

Figure 6: Fuel mass loss plotted as a function of the calculated gravity current velocity. The uncertainty of each measurement was estimated from the law of propagation of uncertainty.

4. Conclusions

This work highlights the effects of water suppression on the backdraft phenomenon. Adding water within an enclosure reduces the normalized positive density difference that slows the gravity current flow into a compartment, allowing more fuel to escape and reducing the intensity of a backdraft. It can be inferred that extending the spray time beyond 44.0 s would slow the gravity current velocity such that no backdraft would be observed. The limitations of the internal density were also shown to bound the gravity current velocity, suggesting that backdraft intensity is limited. Future work will focus on other components that may affect the backdraft intensity limitations including spark location, fuel type, and total fuel concentration within the compartment before an anticipated backdraft.

References

[1] C. M. Fleischmann and Z. Chen, Defining the difference between backdraft and smoke explosions, Procedia Engineering 62 (2013) 324–330.

[2] G. E. Gorbett, R. Hopkins, and P. Kennedy, The current knowledge & training regarding backdraft, flashover, and other rapid fire progression phenomena, Annual Meeting of the National Fire Protection Association (2007).

[3] G. Guigay, D. Gojkovic, L.-G. Bengtsson, B. Karlsson, and J. Eliasson, The use of CFD calculations to evaluate fire-fighting tactics in a possible backdraft situation, Fire Technology 45 (2009) 287–311.

[4] D. Gojkovic, Initial backdraft experiments, tech. rep. Report No. 3121, Lund University, 2000.

[5] L. Tsai and C. Chiu, Full-scale experimental studies for backdraft using solid materials, Process Safety and Environmental Protection 91 (2013) 202–212.

[6] J. Park, C. Oh, B. Choi, and Y. Han, Computational visualization of the backdraft development process in a compartment, Journal of Visualization 18 (2015) 25–29.

[7] S. Ferraris, J. Wen, and S. Dembele, Large eddy simulation of the backdraft phenomenon, Fire Safety Journal 43 (2008) 205–225.

[8] J. Park, C. Oh, Y. Han, and K. Do, Computational study of backdraft dynamics and the effects of initial conditions in a compartment, Journal of Mechanical Science and Technology 31 (2017) 985–993.

[9] W. Weng and W. Fan, Experimental study on the mitigation of backdraft in compartment fires with water mist, Journal of Fire Sciences 20 (2002) 259–278.

[10] C. Fleischmann, *Backdraft phenomena*, PhD thesis, University of California, Berkeley, Berkeley, USA, 1993.

[11] C. Fleischmann, P. Pagni, and R. Williamson, Quantitative backdraft experiments, Fire Safety Science-Proceedings of the Fourth International Symposium (1994), pp. 337–348.

[12] C. Fleischmann, P. Pagni, and R. Williamson, Exploratory backdraft experiments, Fire Technology 29 (1993) 298–316.

[13] D. Gottuk, M. Peatross, J. Farley, and F. Williams, The development and mitigation of backdraft: a real-scale shipboard study, Fire Safety Journal 33 (1999) 261–282.

[14] D. Gottuk, F. Williams, and J. Farley, The development and mitigation of backdrafts: a full-scale experimental study, Fire Safety Science 5 (1997) 935–946.

[15] W. Weng and W. Fan, Experimental study of backdraft in a compartment with different opening geometries and its mitigation with water mist, Fire Safety Science-Proceedings of the 8th International Symposium (2005), pp. 1181–1192.

[16] W. Weng, W. Fan, and Y. Hasemi, Prediction of the formation of backdraft in a compartment based on large eddy simulation, Engineering Computations 22 (2005) 376–392.

[17] N. Chen, *Smoke Explosion in Severally Ventilation Limited Compartment Fires*, MA thesis, University of Canterbury, Christchurch, New Zealand, 2012.

[18] J. Gong, L. Yang, X. Chen, and Z. Guo, Theoretical analysis of the backdraft phenomena induced by liquid fuel, Chinese Science Bulletin 51 (2006) 364–368.

[19] C. Brown, R. Falkenstein-Smith, and T. Cleary, Reduced-Scale Compartment Gaseous Fuels Backdraft Experiments, NIST Technical Note Report No. 2183, National Institute of Standards and Technology, 2021.

[20] R. Falkenstein-Smith and T. Cleary, Thermal and gas mixture composition measurements preceding backdrafts in a $2/5^{th}$ scale compartment, NIST Technical Note Report No. 2185, National Institute of Standards and Technology, 2022.

[21] V. Babrauskas, W. Parker, G. Mulholland, and W. Twilley, The phi meter: A simple, fuel-independent instrument for monitoring combustion equivalence ratio, Review of Scientific Instruments 65 (1994) 2367–2375.

[22] R. Falkenstein-Smith and T. Cleary, The Design and Performance of a Second-Generation Phi Meter, NIST Technical Note Report No. 2184, National Institute of Standards and Technology, 2021.

[23] R. Falkenstein-Smith, K. Harris, K. Sung, T. Liang, and A. Hamins, A calibration and sampling technique for quantifying the chemical structure in fires using GC/MSD analysis, Fire and Materials 46 (2021) 3–11.

[24] R. Falkenstein-Smith, K. Sung, J. Chen, and A. Hamins, The chemical structure of a 30 cm methanol pool fire, Fire and Materials 45 (2021) 429–434.

[25] R. Falkenstein-Smith, K. Sung, J. Chen, and A. Hamins, Mixture fraction analysis of combustion products in medium-scale pool fires, Proceedings of the Combustion Institute 38 (2021) 4935–4942.

[26] R. L. Falkenstein-Smith, K. Sung, and A. Hamins, Characterization of Medium-Scale Propane Pool Fires, Fire Technology (2023) 1–18.

[27] R. Bryant, T. Ohlemiller, E. Johnsson, A. Hamins, B. Grove, W. Guthrie, A. Maranghides, and G. Mulholland, The NIST 3 megawatt quantitative heat release rate facility, NIST Special Publication Report No. 1001, National Institute of Standards and Technology, 2003.

[28] M. Hurley, ed., SFPE Handbook of Fire Protection Engineering, 5th, Springer, New York, 2016.

[29] R. Falkenstein-Smith, K. Sung, J. Chen, K. Harris, and A. Hamins, The Structure of Medium-Scale Pool Fires, Second Edition, NIST Technical Note Report No. 2082,e2, National Institute of Standards and Technology, 2021.

[30] W. Weng, W. Fan, J. Qin, and L. Yang, Study on salt water modeling of gravity currents prior to backdrafts using flow visualization and digital particle image velocimetry, Experiments in Fluids 33 (2002) 398–404.